Electronic Supplementary Material (ESI) for Nanoscale Advances.

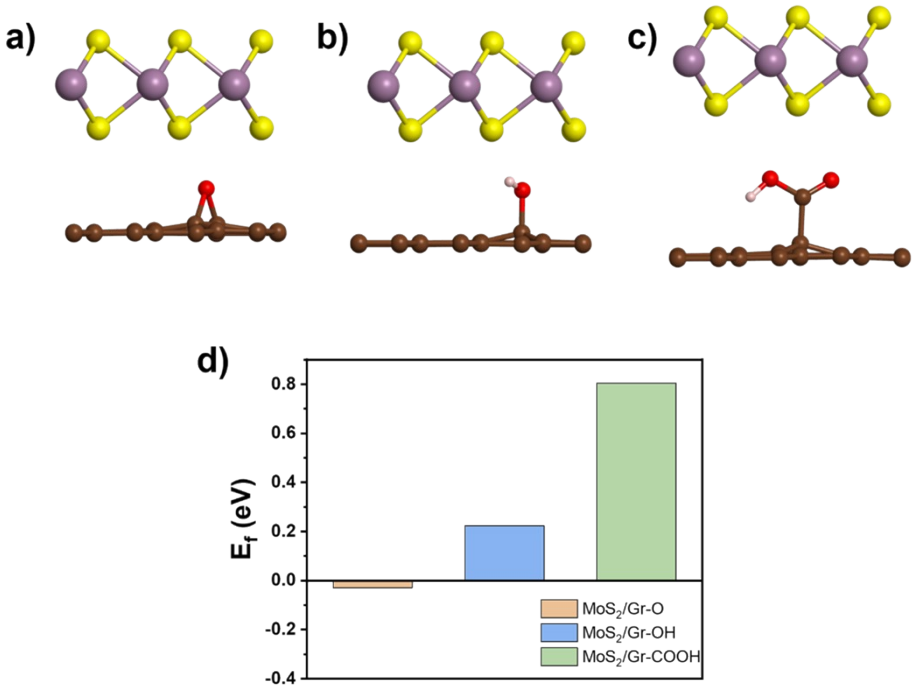

Figure S1. | Side view of functional groups upward structures for (a) MoS_2/Gr-O, (b) MoS_2/Gr-OH and (c) MoS_2/Gr-COOH. Mo, S, C, O, H atoms are colored as violet, yellow, brown, red, and white, respectively, and (d) formation energy (E_f) of each heterogeneous bilayer.

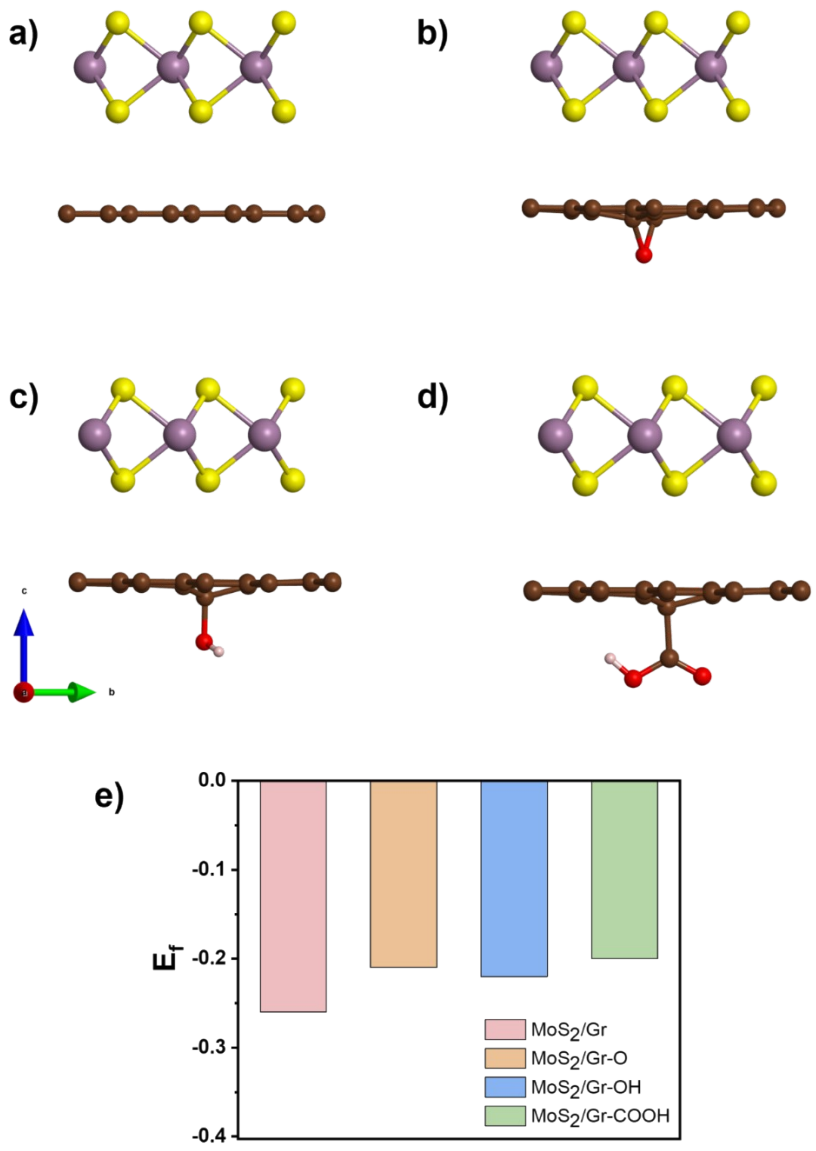

Figure S2. | Side view of the optimized heterogeneous bilayers of (a) MoS_2/Gr, (b) MoS_2/Gr-O, (c) MoS_2/Gr-OH and (d) MoS_2/Gr-COOH. (e) formation energy (E_f) of each heterogeneous bilayer.

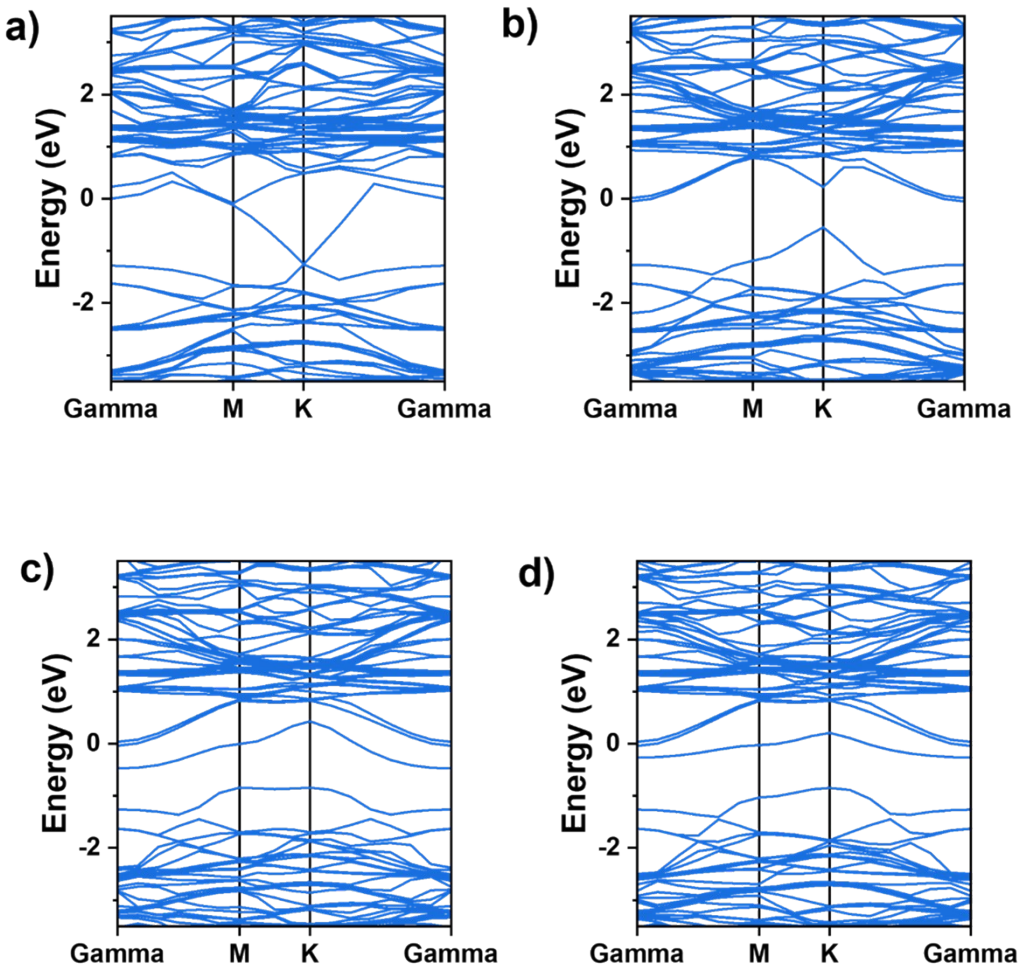

Figure S3. | Electronic structure: band structure plot of (a) MoS_2/Gr, (b) MoS_2/Gr-O, (c) MoS_2/Gr-OH, and (d) MoS_2/Gr-COOH.

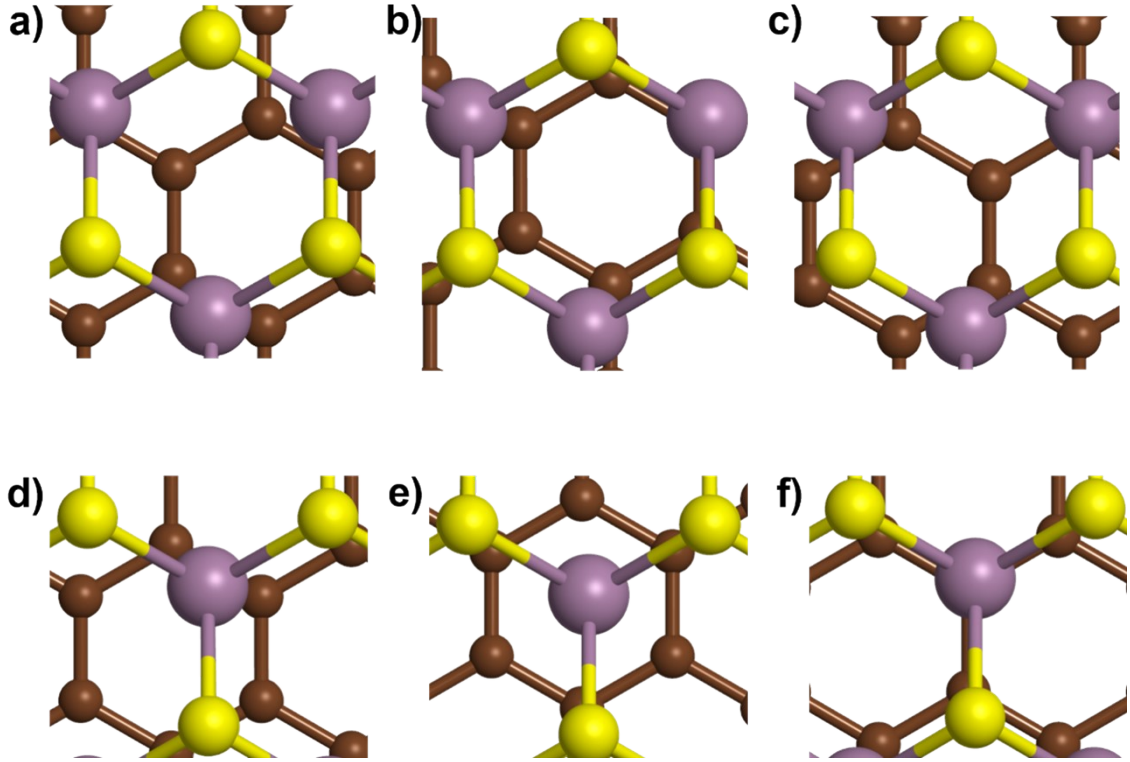

Figure S4. | Top view of the all the possible Na adsorption sites at MoS_2/Gr heterointerfaces. (a) hollow-bridge, (b) hollow-hollow, (c) hollow-atop, (d) atop-Bridge, (e) atop-hollow, and (f) atop-atop.

Table S1. Different sodium intercalation sites as shown in **Figure S4**.

Hollow	**Top**
hollow (MoS_2) – bridge (Graphene)	atop (MoS_2) – bridge (Graphene)
hollow (MoS_2) – hollow (Graphene)	atop (MoS_2) – hollow (Graphene)
hollow (MoS_2) – atop (Graphene)	atop (MoS_2) – atop (Graphene)

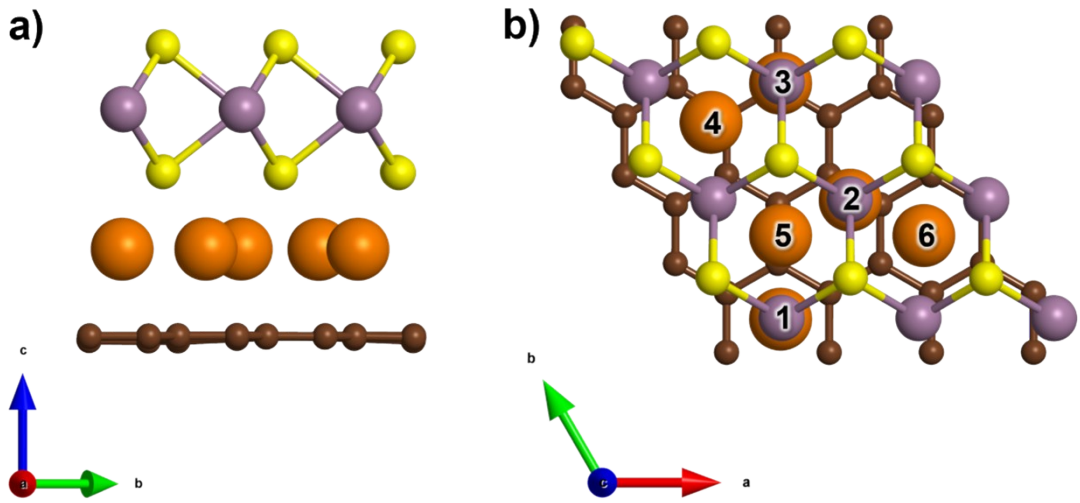

Figure S5. | (a) Side and (b) top views of interface for MoS_2/Gr marked with 6 possible Na (marked as orange) adsorption sites. (Each number corresponds to possible Na intercalation sites of details are shown in the **Table S2**)

Table S2. | Sodium binding energy, ΔE_b (eV), and interlayer distance, ***d*** **(Å)**, at different intercalation sites described in **Figure S5**.

Adsorption site	ΔE_b **(eV)**	***d*** **(Å)**
Top-Hollow (1)	-0.63	3.95
Top-Bridge (2)	-0.53	4.07
Top-Top (3)	-0.52	4.01
Hollow-Top (4)	-0.51	4.07
Hollow-Bridge (5)	-0.51	4.07
Hollow-Hollow (6)	-0.60	3.98

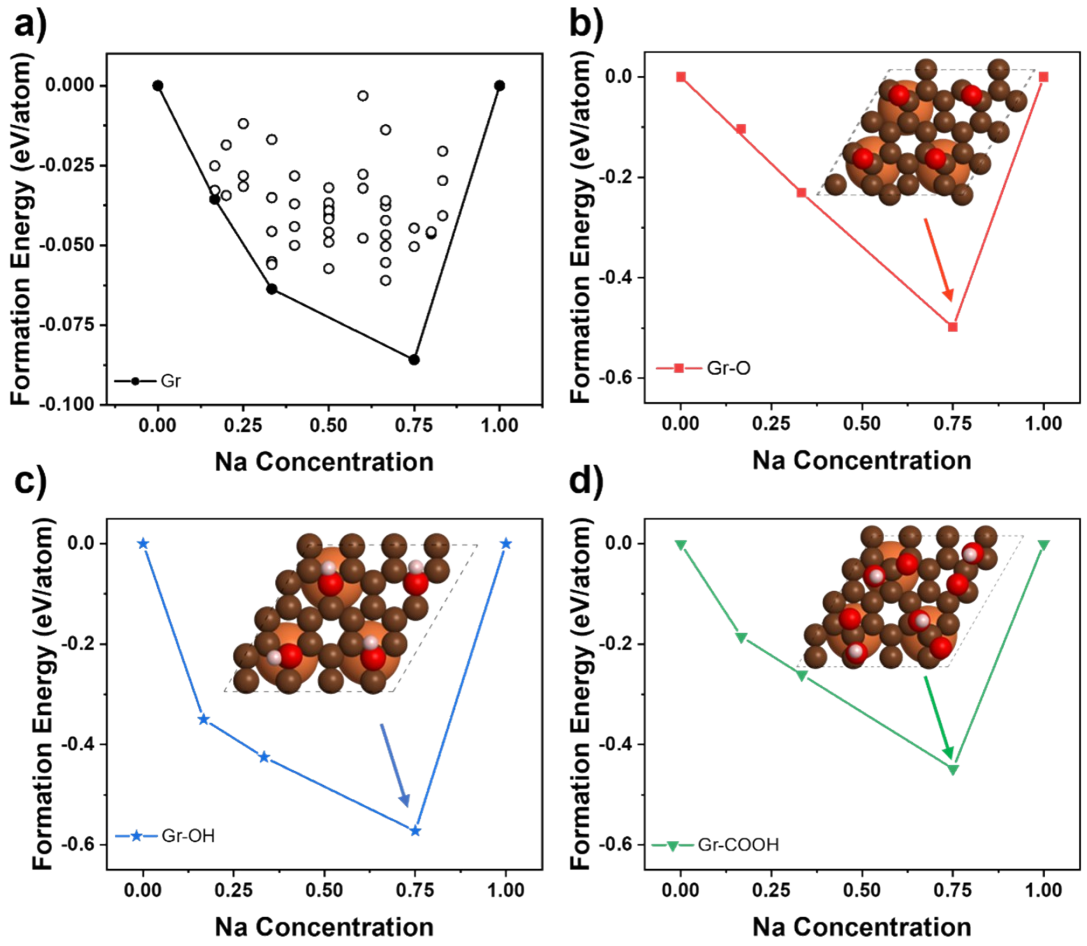

Figure S6. | Energy convex hull of the formation energy as a function of Na concentration in a single layer. (a) graphene, (b) Gr-O, (c) Gr-OH, and (d) Gr-COOH.

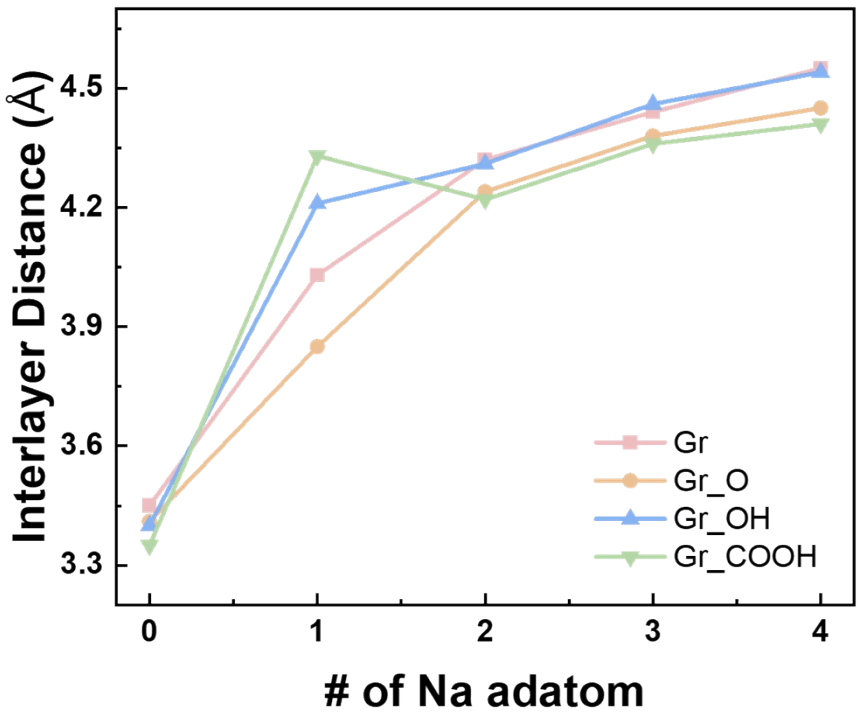

Figure S7. | Interlayer distance of MoS_2/Gr and MoS_2/rGO with respect to intercalated Na atom number.

Table S3. | Interlayer expansion in z-direction after sodium intercalation associated with heterogeneous bilayers.

Heterogeneous Bilayer	Interlayer Expansion (After Na Intercalation)
MoS_2/Gr	12.9 %
MoS_2/Gr-O	15.5 %
MoS_2/Gr-OH	6.8 %
MoS_2/Gr-COOH	4.5 %

Carbon vacancy effect

In the graphene modified with various oxygen functional groups, mono-carbon defect was created to analyze its effect on the Na intercalation process on the aspect of Na affinity, diffusion behavior and working potential. Na intercalation energies were evaluated as -1.25, -1.06, -1.21, and -1.21 eV in MoS_2/Gr, MoS_2/Gr-O, MoS_2/Gr-OH and MoS_2/Gr-COOH, respectively. The calculations indicate that the carbon defects render the Na intercalation energies over model systems with different oxygen functional groups negligible, which was considerable in defect-free models. It implies that the effect of carbon vacancies is more pronounced than that of the oxygen functional groups on Na affinity.

The carbon vacancies can trap Na atoms not only to increase Na affinity but also to increase activation barrier for Na diffusion. It was known that the diffusion energy barrier between the initial state and the saddle point is notably higher in the presence of vacancies than without them (Supplementary Table S4), delaying diffusion process.

We analyzed the influence of vacancies on the OCV and observed that the initial potential is similar regardless of being the oxygen functional groups. The superior binding energy of defected MoS_2/Gr to defected MoS_2/rGO is reflected in its higher OCV. As the concentration of Na increases, however, the adsorptive properties of MoS_2/rGO begin to dominate, leading to an increase in OCV above that of MoS_2/Gr. It implies that while carbon vacancies can increase Na binding energy the stronger attraction by rGO plays more significant role in the working potential of Na intercalation.

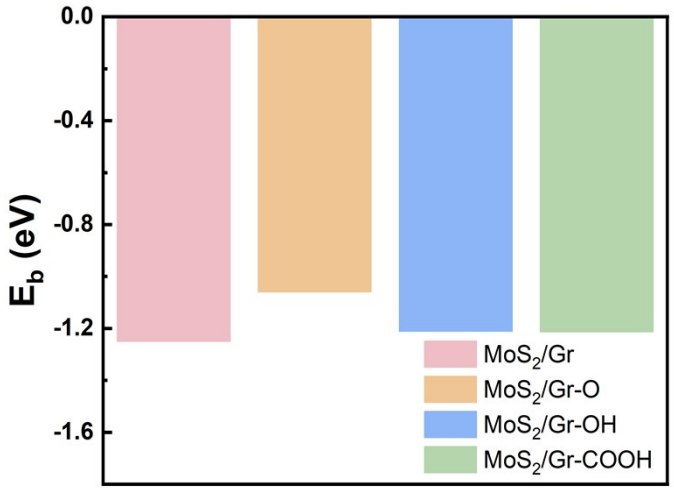

Figure S8. Na binding energy (E_b) of carbon defected MoS_2/rGO heterogeneous bilayer.

Table S4. The activation energy of MoS_2/Gr, MoS_2/Gr-O, MoS_2/Gr-OH, and MoS_2/Gr-COOH

Heterogeneous Bilayer	Activation Barrier (eV)
MoS_2/Gr	0.32
MoS_2/Gr-O	0.43
MoS_2/Gr-OH	0.45
MoS_2/Gr-COOH	0.41

Table S5. The band gap of the MoS_2/rGO changes according to the number of oxygen functional groups.

# of Functional Group	1	2	3	4
MoS_2/Gr-O	0.58	0.608	0.62	0.65
MoS_2/Gr-OH	0.68	0.697	0.698	0.712
MoS_2/Gr-COOH	0.61	0.648	0.681	0.71

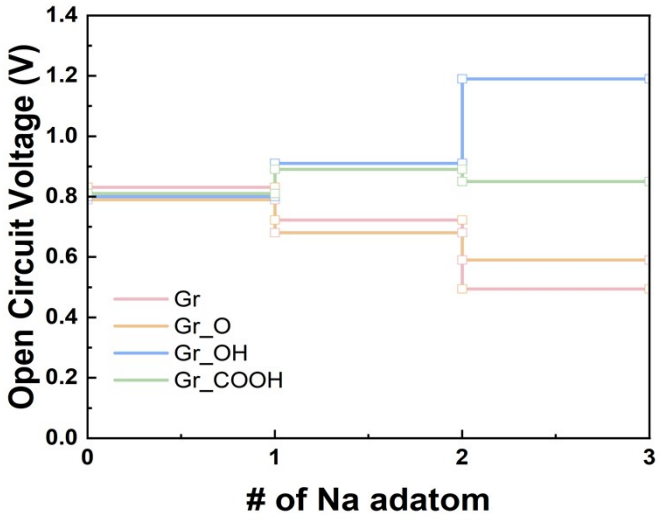

Figure S9. The voltage profile carbon defected MoS_2/Gr and MoS_2/rGO as a function of Na adatom number.

Table S6. The formation energy of MoS_2/Gr, MoS_2/Gr-O, MoS_2/Gr-OH, and MoS_2/Gr-COOH as a function of the number of Na atoms

# of Na atoms	Pristine	1	2	3	4
MoS_2/Gr	-0.26	-0.89	-0.35	-0.21	-0.1
MoS_2/Gr-O	-0.21	-0.66	-0.61	-0.52	-0.44
MoS_2/Gr-OH	-0.23	-0.81	-0.75	-0.74	-0.59
MoS_2/Gr-COOH	-0.2	-0.77	-0.76	-0.73	-0.61